Mid-IR spectra of different conformers of phenylalanine in the gas phase

G. von Helden,*[a] I. Compagnon,[b] M. N. Blom,[b] M. Frankowski,[a] U. Erlekam,[a] J. Oomens,[b] B. Brauer,[c] R. B. Gerber[cd] and G. Meijer[a]

Received 29th August 2007, Accepted 13th November 2007
First published as an Advance Article on the web 29th November 2007
DOI: 10.1039/b713274c

The experimental mid- and far-IR spectra of six conformers of phenylalanine in the gas phase are presented. The experimental spectra are compared to spectra calculated at the B3LYP and at the MP2 level. The differences between B3LYP and MP2 IR spectra are found to be small. The agreement between experiment and theory is generally found to be very good, however strong discrepancies exist when $-NH_2$ out-of-plane vibrations are involved. The relative energies of the minima as well as of some transition states connecting the minima are explored at the CCSD(T) level. Most transition states are found to be less than 2000 cm^{-1} above the lowest energy structure. A simple model to describe the observed conformer abundances based on quasi-equilibria near the barriers is presented and it appears to describe the experimental observation reasonably well. In addition, the vibrations of one of the conformers are investigated using the correlation-corrected vibrational self-consistent field method.

1. Introduction

To understand the structure and dynamics of biological molecules in their native environments, it is often imperative to first understand these properties for the isolated systems in the gas phase. There, one can measure the intrinsic properties and it is indeed frequently observed that they differ considerably from those observed when the molecule is in solution, embedded in a solid or deposited on surfaces. The differences can be explained in terms of the various bonding, electrostatic and dispersion interactions with the environment, which can—and will—affect the properties of the molecules.[1] Nonetheless, gas-phase studies can be used to deduce subtle structural parameters of relevant biological systems.[2]

It is frequently observed that even small systems, such as isolated amino-acids in the gas phase, have complex potential energy surfaces with many local minima that are often simultaneously populated. In the 1980s, experiments using UV hole burning techniques coupled to molecular beam methods demonstrated that different conformers of simple amino-acids can be selectively excited and investigated.[3] When coupled to a tunable infrared (IR) laser, this hole-burning spectroscopic method allows the recording of conformer-specific IR spectra in a heterogeneous mixture of conformations.[4] The IR absorption spectra uniquely identify the structure: line intensities and frequencies give direct information on the forces that hold the molecule together. Coupled with DC electric fields, experiments can even allow for the measurement of the direction of the transition dipole moment.[5] Conformer selective IR spectroscopy in the gas phase has been applied to various interesting systems, such as isolated or paired nucleobases,[6] to the amino-acids phenylalanine[4] and tryptophan,[7,8] to beta-sheet model systems[9] and other small peptides.[10,11] Most of these experiments have been performed using laser systems that cover the near- and mid-IR and are limited to wavelengths shorter than about 7 μm. In this range X–H (X = C, O, N) and C=O stretching vibrations are probed and the experiments provide an insight into the conformational arrangement, as those vibrational transitions exhibit shifts in absorption frequency and changes in intensity in the presence of, for instance, intramolecular hydrogen bonds or solvating molecules.

However, most vibrational modes have characteristic frequencies that lie further in the IR and are not accessible using standard laser systems. These low frequency modes are frequently floppy, large amplitude motions and delocalized vibrations which can be of particular importance in the dynamics of conformational change. These delocalized modes are often also more diagnostic as they appear to be more conformer specific. This has led to a renewed interest in the far-IR (or THz) spectroscopy of biomolecules, though particularly in the condensed phase.[12,13] This complicates the interpretation of these spectra as intermolecular and 'phonon' modes occur abundantly in this range. Using a free electron laser, such spectra can be obtained in the gas phase, where the intrinsic molecular THz spectrum may be obtained. We should also mention that it is often found that the agreement with computed spectra (using a harmonic frequency approximation) is in general less favorable than for the more local modes at shorter wavelengths. Recently, specialized tabletop systems[14] and free electron lasers[15] have shown to be suitable tools for experiments in the low frequency range on gas-phase biomolecules.[8]

In many biomolecules, a conformational change can be induced thermally and the barriers that are crossed in such

[a] *Fritz-Haber-Institut der Max-Planck-Gesellschaft, Faradayweg 4-6, D-14195 Berlin, Germany. E-mail: helden@fhi-berlin.mpg.de*
[b] *FOM Institute for Plasmaphysics, Edisonbaan 14, NL-3439 MN Nieuwegein, The Netherlands*
[c] *Fritz Haber Molecular Dynamics Research Center, The Hebrew University of Jerusalem, Jerusalem, Israel*
[d] *Department of Chemistry, University of California, Irvine, CA 92797, USA*

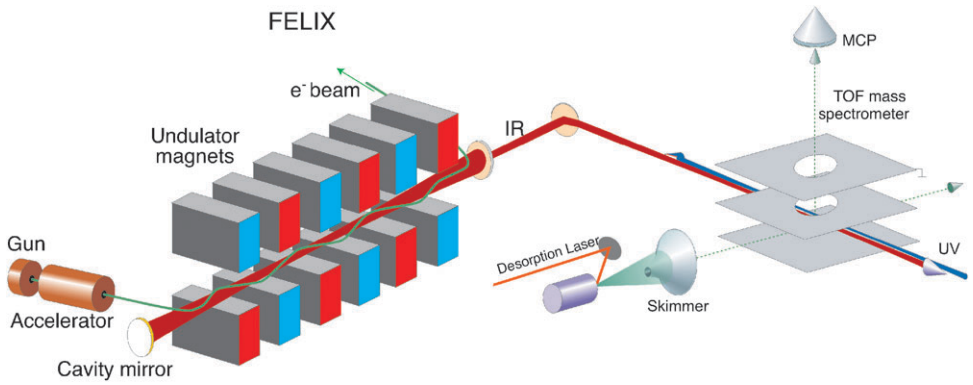

Fig. 1 Experimental setup to perform IR spectroscopy on gas-phase biomolecules using the free electron laser FELIX. See text for details.

processes thus have heights that are comparable to the energy of IR photons. In most experiments, the local minima are investigated and only little information is available on the barriers that separate those minima. In recent experiments, Zwier and coworkers showed that conformational change in gas-phase biomolecules can be induced by the absorption of 3 μm photons and that this change can be monitored by UV excitation methods.[16] However, the barriers that separate the different conformations are much lower in energy than the 3 μm excitation energy. Information on their height can be obtained by populating lower lying levels *via* stimulated emission pumping (SEP).[17]

Here, we present mid-infrared (mid-IR) spectra of six conformers of the amino-acid phenylalanine in the gas phase. The experimental spectra are augmented by calculated spectra at the B3LYP and the MP2 level. The transition states that separate the various conformers are investigated using theory and a simple model for the observed conformer abundances is presented. In addition, the role of anharmonic corrections to the calculated vibrational frequencies is investigated and discussed.

2. Experimental

The experimental setup consists of a pulsed molecular beam apparatus equipped with a laser desorption source coupled to a time-of-flight (TOF) mass spectrometer and has been described earlier.[8,18] The sample is mixed with graphite powder, rubbed onto a graphite bar and placed directly beneath the nozzle of the pulsed valve, through which neon or argon with a backing pressure of 3 bars is expanded as a buffer gas. The molecules are desorbed from the sample using a $\sim$1 mJ laser pulse at 1064 nm, which is synchronized with the opening of the pulsed valve in order to achieve an efficient internal cooling in the supersonic expansion of the rare-gas beam. The neutral molecular beam is skimmed and enters the extraction region of the TOF mass spectrometer. The molecules are ionized with a tunable UV laser beam (frequency doubled output of a dye laser pumped with the third harmonic of a Nd:YAG laser) crossing the molecular beam perpendicularly. The ions are detected on a microchannel plate detector and the TOF transient is recorded and averaged using a digital oscilloscope. Vibrational spectroscopy is performed using the infrared radiation produced by the free electron laser for Infrared experiments (FELIX),[15] described below. The IR laser beam is aligned perpendicularly to the molecular beam and counter propagating to the UV beam. A scheme of the setup is shown in Fig. 1.

Ionization of the molecules is performed *via* a resonant 1-color 2-photon process (R2PI) around 260 nm and IR spectra are obtained *via* IR ion dip spectroscopy[4,19–21] The UV-excitation laser is then parked on the S_1–S_0 transition of the conformer of interest, and the IR laser, which is fired in time and position just before the UV laser, is scanned over the fingerprint region of the molecule (300–1900 cm^{-1}). At each IR wavelength, the signal obtained when FELIX is irradiating the molecular beam is divided by the signal obtained without FELIX and the natural logarithm is taken. The FELIX fluence is not constant over the range scanned in this experiment, and the IR spectra are linearly corrected for this.

Due to its characteristics, FELIX is uniquely suited for gas-phase experiments. It is continuously tunable over the 5–250 μm range. At a given setting of the beam energy, however, the tuning range is limited to about a factor of three in wavelength. Hence, at a given electron beam setting, the range from 5 to 15 μm, for example, can be continuously scanned within a few minutes. The macropulse length is 5 μs and the repetition rate can be up to 10 Hz (5 Hz is used in the present experiment). The micropulse length can be adjusted and ranges from 300 fs to several ps. The bandwidth is transform limited and can range from 0.5% FWHM of the central wavelength to several percent. The micropulse repetition rate can be selected to be either 25 MHz or 1 GHz, resulting in a micropulse spacing of 40 or 1 ns, respectively. In the 1 GHz mode, the output energy can be up to 100 mJ per macropulse.

3. Results and discussion

3.1 UV spectrum

Phenylalanine can be brought into the gas phase *via* laser desorption and can be examined using UV and IR lasers. Adiabatic cooling with a neon buffer gas in the molecular beam expansion causes the molecule to vibrationally and rotationally cool to temperatures between 2 and 20 K. When only using the UV laser, an R2PI spectrum, as shown in Fig. 2, can be obtained. This spectrum is very similar to spectra obtained when bringing phenylalanine into the gas phase *via*

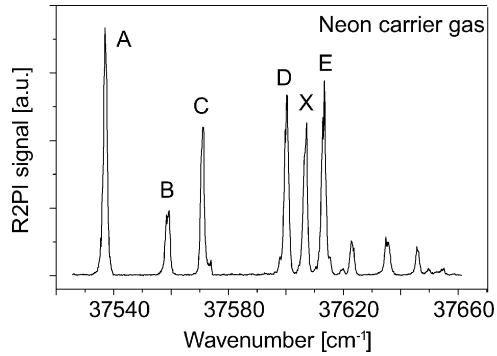

Fig. 2 UV-resonant 2 photon ionization (R2PI) spectrum of jet-cooled phenylalanine. The peaks labeled A–E as well as X result from different conformers. The labeling is the same as in ref. 4.

heating, followed by cooling in a molecular beam, as performed by Levy *et al.*[22] and Simons, Snoek and coworkers.[4] *Via* hole-burning experiments, it has been shown that the peaks in the UV spectrum can be attributed to a distribution of conformers. In ref. 4 and 22, a labeling scheme is used which we will adopt here as well. In the wavelength range shown here, all major peaks in the UV spectrum belong to different conformers, which are labeled A, B, C, D, X and E.[4] Outside this range, towards higher wavenumbers, peaks resulting from three other conformers are observed.[4] As has been recognized by Simons *et al.*, conformer "X" is only observable in R2PI spectra and is not observed in laser induced fluorescence (LIF) spectra.[22]

It is difficult to deduce structural information by only considering low resolution UV spectra, such as the one shown here. Some information can be obtained from, for example, the conformer specific measurement of the dispersed fluorescence[22] or the ionization potential.[23] In addition, the comparison of calculated and measured high resolution, *i.e.* (partially) rotationally resolved, UV spectra can facilitate a structural assignment.[24] However, the most versatile method to deduce structural information on the conformers of phenylalanine and similar systems remains conformer specific IR spectroscopy, either in the X–H stretch (X = C, N, O) region around 3 μm[4] or in the fingerprint region beyond 5 μm.[8]

3.2 IR spectra

When the UV excitation and ionization laser is parked on one of the UV transitions in Fig. 2, the IR spectrum of the corresponding conformer can be measured *via* ion dip spectroscopy. In Fig. 3, the IR spectra of six conformers are shown. The spectra for conformers X, D and A were measured in the range from 300–1900 cm^{-1}, while the spectra of B, C and E were only measured in the 500–1900 cm^{-1} range. Clearly, in all spectra, distinct peaks can be recognized having widths ranging from 3–5 cm^{-1} in the lower wavenumber region, up to 20 cm^{-1} around 1800 cm^{-1}. Those widths are comparable to the corresponding width of the infrared laser.

The spectra of the six conformers clearly differ from each other. Nonetheless, they fall into two groups: the spectra of conformers B and X resemble each other and are qualitatively different from those of conformers D, C, E and A. Near 1800 cm^{-1}, each spectrum shows a peak that can be assigned

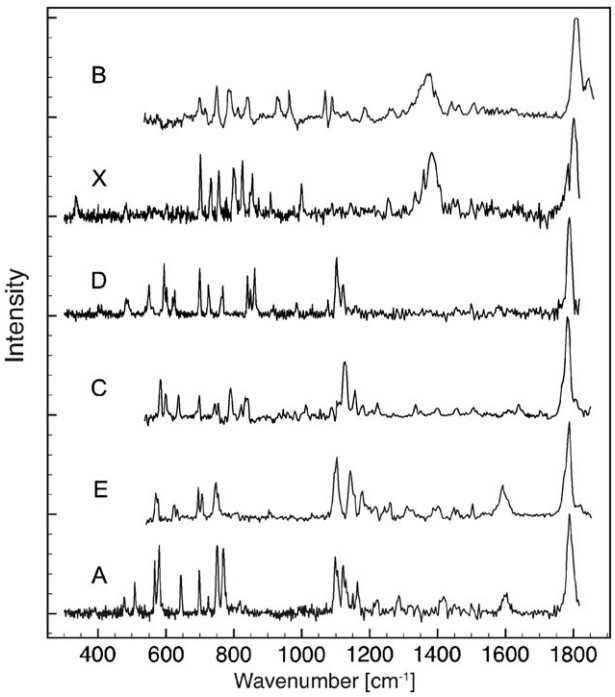

Fig. 3 IR spectra of six conformers of phenylalanine. They are obtained by measuring the IR-UV ion dip spectra with the UV laser parked on the corresponding resonance in the UV-R2PI spectrum (Fig. 2).

to the excitation of the C═O stretching mode. For B and X, these peaks are found at 1808 and 1798 cm^{-1}, respectively, while for D, C, E and A, they are shifted to the red and are found at 1787, 1781, 1785 and 1787 cm^{-1}, respectively. The absolute accuracy of these values is estimated to be about ±10 cm^{-1} while the relative accuracy is about ±5 cm^{-1}.

Hydrogen bonding can shift the C═O stretching frequency to the red and it seems plausible that in D, C, E and A, the C═O group is involved in H-bonding while this group is free in B and X. This is in agreement with previous structural assignments.[4,24] Further structural information can be deduced from the broad peaks near 1350 cm^{-1} in the spectra of conformers B and X as well as from the group of peaks between 1100 and 1150 cm^{-1} in the spectra of D, C, E and A. These peaks can be assigned to C–O–H bending modes (coupled to C–OH stretching motion). When the H-atom of the COH group is involved in H-bonding, the C–O–H bending frequency usually shifts to the blue. It thus seems likely that the H atom of the COH group in B and X is involved in a "strong" H-bond. The observed spectra are thus compatible with structures proposed previously[4,24] and shown in Fig. 4. For X and B, the H-atom of the COOH group is H-bonded to the N-atom of the NH_2 group and the C═O group is free, while for D, C, E and A, the H-atoms of the NH_2 group have a H-bond to the C═O group and the C–O–H is not involved in H-bonding.

3.3 Computed IR spectra

The structures and IR spectra of 14 conformers are calculated both at the B3LYP/6-311++G(2d,p) as well as at the MP2/6-311+G(2df,2p) level. In addition, single point energy

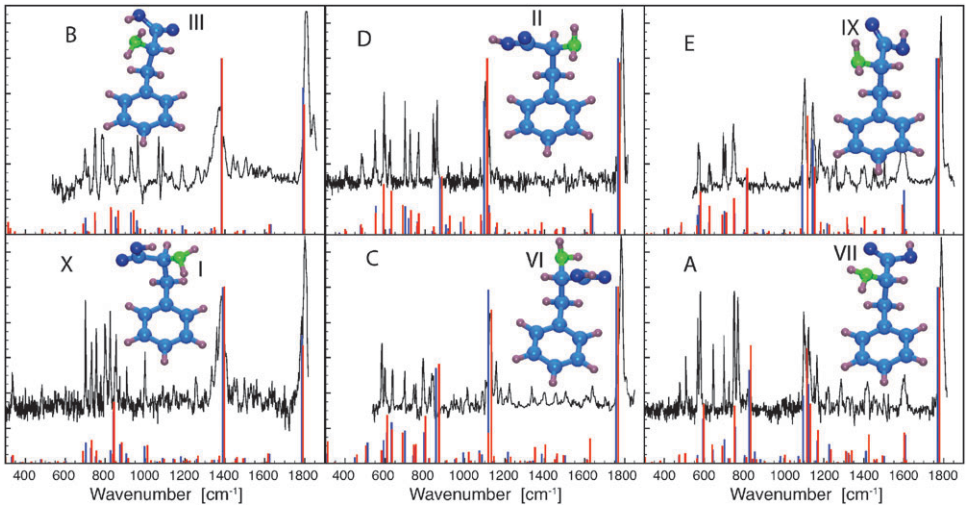

Fig. 4 Experimental IR spectra of six phenylalanine conformers, compared to theoretical stick spectra calculated at the B3LYP/6-311++(2d,p) level (blue) as well as calculated at the MP2/6-311G+(2df,2p) level (red). All theoretical data is scaled by multiplying the theoretical frequencies by 0.98. For all structures, the differences between the B3LYP and MP2 results are small.

calculations are performed at the CCSD(T)/6-311+G(2df,2p) level, using the MP2 optimized structure. Their relative energies can be found in Table 1. The structures considered include the nine lowest energy structures by Snoek *et al.*[4,24] (labeled I–IX), three additional low energy structures by Kaczor *et al.*[25] (labeled IIIb1, IIIb2 and IIIc1) as well as two low energy structures by Huang *et al.*[26] (labeled H8 and H10).

The calculated IR spectra can be compared to the experimental IR spectra. The best overall agreement between theory and experiment is obtained with the assignment of Snoek *et al.*[24] where the spectra of conformers B, X, D, C, E and A are attributed to originate from conformers with structures III, I, II, VI, IX and VII, respectively, and the corresponding spectra are shown in Fig. 4. All peak positions in the calculated spectra are scaled with a uniform factor of 0.98 (*vide infra*). Both, the results from the B3LYP (blue) and the MP2 (red) calculations are shown. For most resonances, the differences between the two spectra are small and it can be concluded that the large computational effort for the calculations of the MP2 frequencies is, at least for the systems considered here, not justified. The agreement between the calculated and experimental spectra is very good, giving confidence in the structures that the calculations are based on. Peaks corresponding to C═O stretching modes around

Table 1 Relative energies (in cm^{-1}) of the various structures and transition states considered

	Structure	B3LYP[a]	MP2[b]	CCSD(T)[b]	ZPE
Minima	I	32.0	0[d]	0[e]	0[f] (0[g])
	II	436.9	281.2	230.5	−133.4(−146.4)
	III	0[c]	273.2	205.2	−27.8 (−17.4)
	IV	105.7	597.6	415.2	−79.4 (−83.2)
	V	694.5	549.4	518.4	−91.2 (−103.1)
	VI	509.9	611.2	504.0	−164.7 (−166.1)
	VII	472.5	776.6	625.6	−169.8 (−175.5)
	VIII	514.5	1003.4	774.8	−200.2 (−214.1)
	IX	571.7	860.3	699.2	−190.8 (−194.1)
	IIIb1	769.2	1025.7	803.4	−189.2 (−183.8)
	IIIb2	834.0	1149.3	974.5	−179.8 (−190.2)
	IIIc1	810.2	957.8	829.4	−161.5 (−178.3)
	H10	881.7	946.3	824.0	−181.9 (−181.0)
	H8	1102.9	924.0	877.5	−192.1 (−202.2)
Transition-states	I–III	1430.0	1911.0	1754.5	−29.2
	I–V	4707.5	4366.5	4268.2	−528.7
	II–V	1481.3	1652.5	1497.1	−119.8
	II–VI	2060.4	2118.0	1991.6	−226.8
	II–VII	2139.6	2539.0	2339.4	−212.3
	III–IV	157.2	672.5	511.6	−125.6
	VI–IX	1362.0	2012.5	1691.6	−208.7
	VII–VIII	1026.4	1464.0	1259.0	−314.7
	VIII–IX	711.2	1191.1	986.4	−273.5

[a] Using the 6-311++G(2d,p) basis set. [b] Using the 6-311+G(2df,2p) basis set. [c] $E = -554.97604568$ a.u. [d] $E = -553.70147861$ a.u. [e] $E = -553.84470161$ a.u. [f] At the B3LYP level 41625.9 cm^{-1} (unscaled). [g] At the MP2 level 42025.9 cm^{-1} (unscaled).

1800 cm^{-1} are predicted a few cm^{-1} to the red from the experiment, irrespective of whether the C=O group is involved in H-bonding (B and X) or not (D, C, E and A). Vibrations originating from the C–O–H bending mode around 1350 cm^{-1} (B and X) or around 1100 cm^{-1} (D, C, E and A) are even better reproduced.

There are however also discrepancies between theory and experiment. All calculations predict $-NH_2$ out of plane bending motion to lie in the frequency range between ~810 and ~925 cm^{-1} (values are scaled by 0.98). This type of motion is quite analogous to that of the umbrella inversion mode in NH_3 or the $-NH_2$ out-of-plane motion in aniline.[27] For those molecules, this motion takes place in a symmetrical double minimum potential with, for aniline, a barrier for inversion of 526 cm^{-1}.[28] Not surprisingly, it could be shown that computations based on the harmonic approximation do not give sensible results[27] for this mode. For phenylanaline, the situation is expected to be similar. A visual inspection of the normal modes in the calculated vibrational spectra shows that many modes between ~810 and ~925 cm^{-1} have contributions from $-NH_2$ motion. In the spectra of Fig. 4, these modes can be observed for VII and IX as the quite intense sticks just above 800 cm^{-1} and they do not have experimental counterparts. For structures II and VI, this motion is less localized in one mode and for structures I and III, this motion is even more mixed with other modes and the corresponding normal vibrations are of relative weak IR intensity.

3.4 Anharmonic calculations

When comparing theoretical to experimental IR spectra, one can notice a good qualitative agreement (see Fig. 4). However, as is common for this type of calculation, the harmonic frequencies were scaled by a factor of 0.98, in order to obtain agreement with experiment.[29] Scaling is usually performed to correct for two shortcomings of the calculations. The first is due to the harmonic approximation used. It is assumed that the vibrations can be described using a purely quadratic potential and that different modes do not couple. In reality, however, the potential is "softer" than a harmonic potential and modes do couple with each other. This will let the calculated frequencies deviate from the experiment, even if the underlying potential energy surface was the "true" one. A second reason is that one might want to correct for deficiencies in the underlying potential. It is, for example, known that in Hartree–Fock calculations, potentials are calculated much too steep and for that reason, such calculations are usually scaled more and factors as small as 0.85 are common.

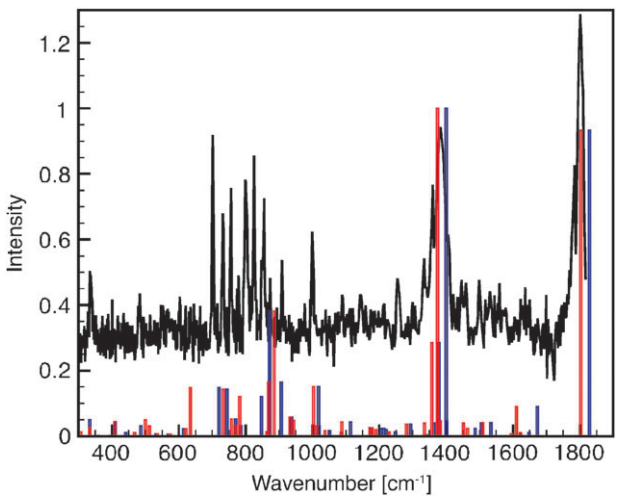

Fig. 5 IR spectrum of phenylalanine conformer X compared to harmonic calculations (blue sticks) and calculations where anharmonic corrections are included (red sticks).

To investigate such effects, anharmonic calculations for phenylalanine conformer X, using the correlation-corrected vibrational self-consistent field (CC-VSCF) method[30–32] were performed. The potential surface used in the calculation was adapted from the PM3 semi-empirical method so that the equilibrium harmonic frequencies would be equivalent to those of a DFT calculation. The resulting harmonic (blue) and anharmonic (red) stick spectra can be seen in Fig. 5. From the comparison, it appears that, in the here considered frequency range, anharmonicities have relatively small effects that shift the harmonic frequencies by about 1–2% to the red. The usage of a scale factor of 0.98 is therefore well justified and the shape of the potentials near the minima is thus well described at the B3LYP/6-311++(2d,p) level, which is used to calculate the spectra in Fig. 4.

However, the effect of anharmonicities can be larger for N–H or O–H stretching modes. The harmonic and anharmonic frequency values for selected modes of conformer X can be found in Table 2. Some modes have an anharmonicity that is much larger than 2%. For example, the NH_2 bending mode has an anharmonicity of 3.9%. Of this, 1.4% are due to (diagonal) single mode anharmonicity and 2.5% due to coupling to other modes. Because of the low intensity of this mode, however, this discrepancy is not apparent in Fig. 4. The N–H and O–H stretching modes have particularly high anharmonicities that can be well above 8%. Additionally, the contribution to the anharmonic frequency due to anharmonicity along a single mode can be positive or negative. In fact, in the region between 1000 and 1400 cm^{-1}, the single mode anharmonic contribution tends to be positive, while the contribution of coupling tends to be negative. This gives a cancellation of effects.

3.5 Potential energy surface and conformer abundances

Important for the dynamics of molecules such as phenylalanine, are the characteristics of barriers that separate different regions in conformational space. For molecules that can be seeded in a molecular beam, elegant experiments can allow one to map out parts of the conformational space and to obtain information about the relevant barriers.[16,17] Unfortunately, it appears that such experiments are much more difficult when laser desorption is used as the method to bring molecules into the gas phase and so far, we were not successful in performing similar experiments on laser-desorbed phenylalanine. However, we present here results from computations that are aimed at further characterizing the potential energy surface and at locating important barriers. The relative energies are given in Table 1 and the structures in Fig. 6 and 7. Several of the transition states have been considered before by others[25] using

Table 2 Harmonic and anharmonic frequencies (wavenumbers in cm^{-1}) for selected modes of conformer X. The harmonic frequencies are calculated at the B3LYP/TZP level and the anharmonic frequencies using the CC-VSCF method. The single mode and coupling contributions (in %) of the anharmonicity are also given

	NH_2 asym. str.	NH_2 sym. str.	O–H str.	C═O str.	NH_2 bend
Harmonic	3605	3506	3433	1829	1673
Anharmonic	3329	3235	3261	1803	1610
Contribution					
Single-mode	0.2	3.2	4.7	0.7	1.4
Coupling	8.5	5.1	0.6	0.8	2.5

different methods and basis sets. The sequence depicted in Fig. 6 corresponds, from left to right, to a clockwise rotation of the amino-acid group around the C_α–$CH_2C_6H_5$ bond, accompanied by a reorientation of the $–NH_2$ group.

Different regions of the conformation space are presented in Fig. 7. Three conformers having an internal OH–NH_2 hydrogen bond as well as the barriers that separate them are shown. The highest transition state at 3740 cm^{-1} separates those structures from structure V, having an NH_2–OH hydrogen bond. A transition state at 1377 cm^{-1} leads from this structure to structure II, and therefore to the conformers depicted in Fig. 6.

In the experiment, it is observed that several conformers are simultaneously present. The final rotational and vibrational temperatures in the molecular beam experiment can be estimated to be a few Kelvin. Thus, considering the energy differences for the various conformers (see Table 1), it is clear that the conformational distribution does not correspond to an equilibrium distribution at the translational or rotational temperature of the molecular beam. What determines the relative populations of the various conformers? Clearly, the experimental conditions as well as the potential energy landscape will play a role. When the molecules are brought into the gas phase (either by evaporation or by laser vaporization), the internal energy is high enough, so that barriers, such as the ones depicted in Fig. 6 and 7 can be crossed. When the internal energy is reduced by collisions, for example, different regions of phase space can become separated. Their relative populations can be estimated by an equilibrium at the height of the barrier that separates them. Such an equilibrium can be estimated using statistical methods, by the ratios of vibrational state densities. Considering the calculations shown in Fig. 6 and 7, for example, one can estimate the relative populations of I, III and IV on one side and II, V–IX on the other, by considering the relative state densities at the energy of 3740 cm^{-1}. Further lowering the energy to 1725 cm^{-1} then, for example, separates I from III and IV and again, their populations can be estimated from the vibrational state densities.

Fig. 8 shows the vibrational state densities as a function of energy for the nine lowest energy structures. The calculations

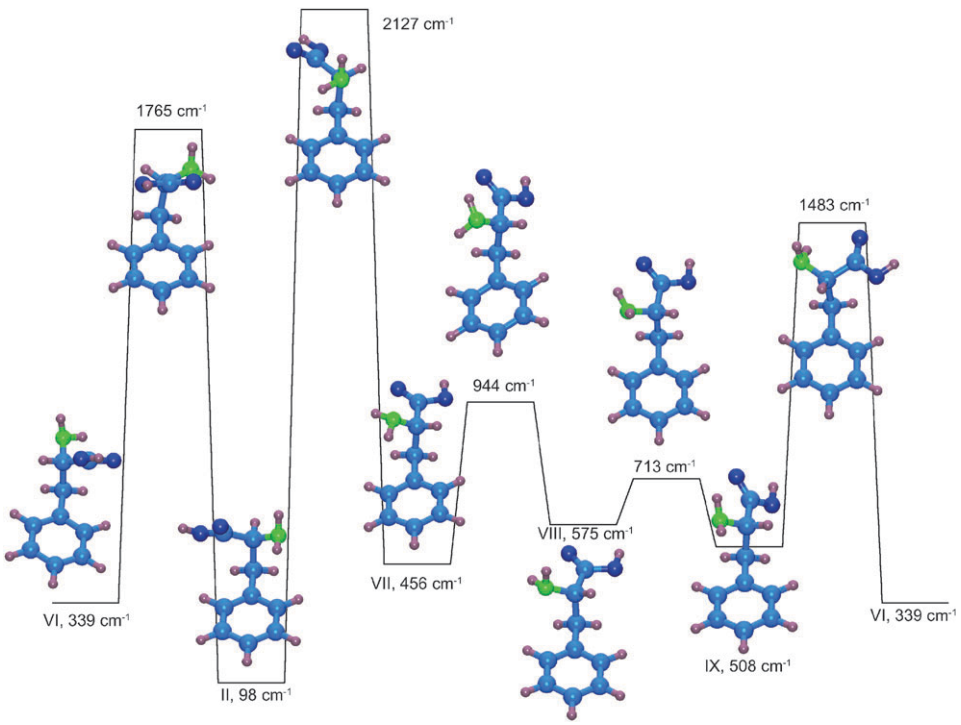

Fig. 6 Structures of six phenylalanine conformers as well as the transition states that separate them, calculated at the MP2/6-311+(2df,2p) level. The transition states are first pre-optimized at the B3LYP/6-311++G(2d,p) level and then refined. A vibrational analysis to verify that they are true first-order saddle points has only been performed at the B3LYP level. The relative energies are the zero-point energy corrected CCSD(T)/6-311+(2df,2p) values (see Table 1).

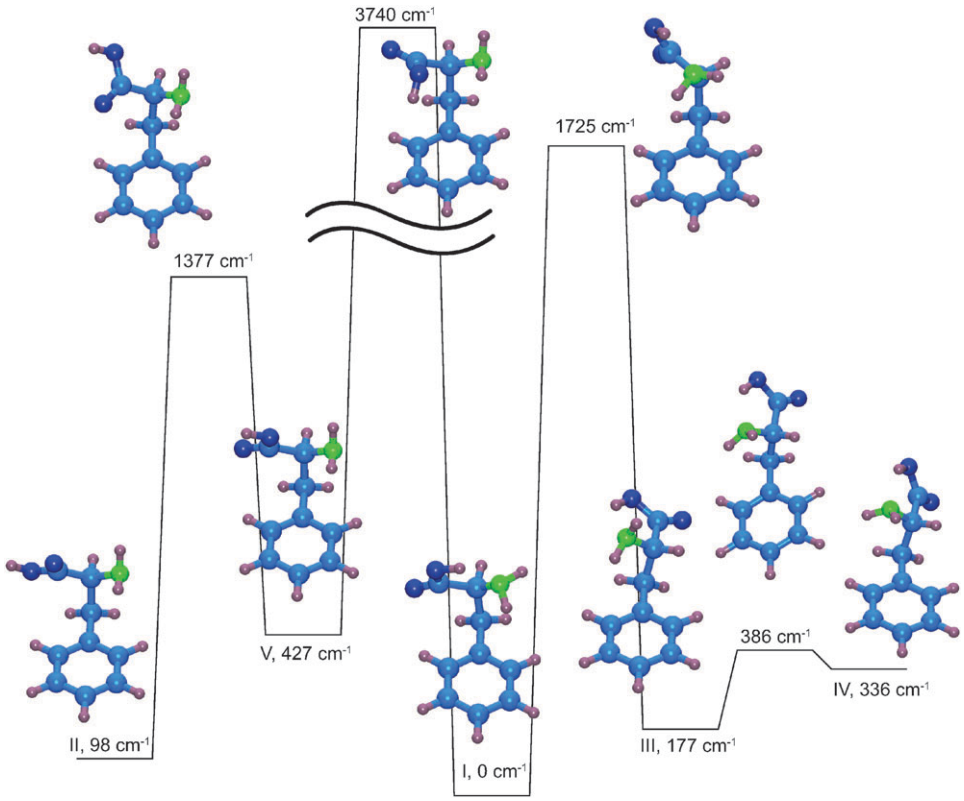

Fig. 7 Structures of five phenylalanine conformers as well as the transition states that separate them, calculated at the MP2/6-311+(2df,2p) level. The transition states are first pre-optimized at the B3LYP/6-311++G(2d,p) level and then refined. A vibrational analysis to verify that they are true first-order saddle points has only been performed at the B3LYP level. The relative energies are the zero-point energy corrected CCSD(T)/6-311+(2df,2p) values (see Table 1).

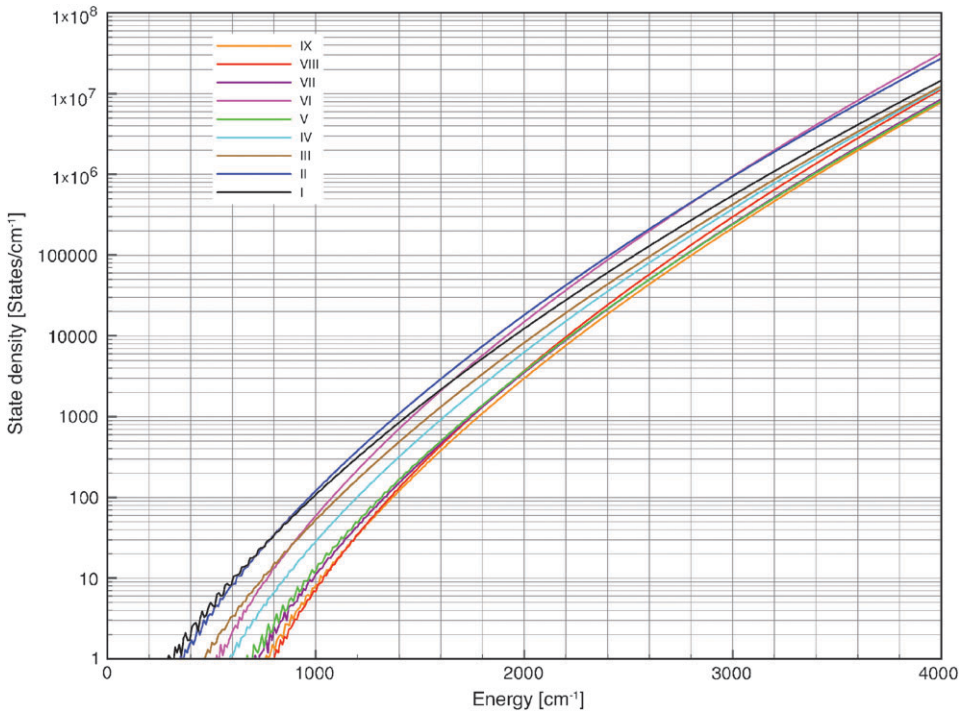

Fig. 8 Densities of vibrational states for the nine lowest energy conformers.

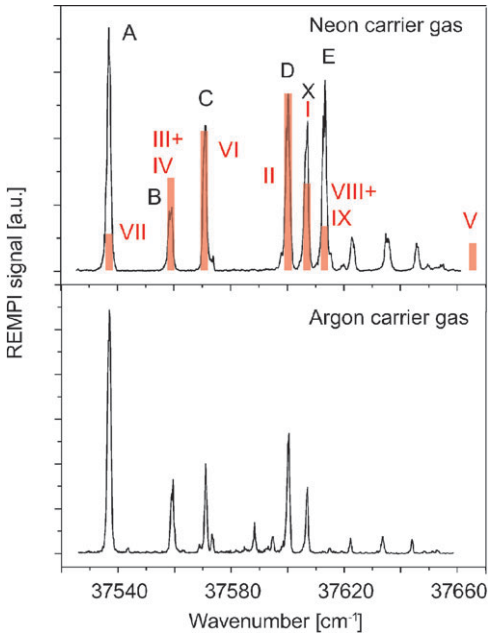

Fig. 9 UV-R2PI spectra of jet-cooled phenylalanine using neon (top) and argon (bottom) as an expansion gas. In the bottom spectrum, conformer E is strongly depleted and A enhanced. Also shown as sticks in the top spectrum are results from a simulation of the intensity distribution.

are performed employing the Beyer–Swinehart algorithm using the B3LYP vibrational frequencies. The relative origins are shifted according to their relative (zero point corrected) CCSD(T) energies. These state densities are used to estimate the relative conformer populations after cooling in the expansion, using the methodology described above. The highest energy barrier of 3740 cm^{-1} separates conformers I, III and IV from II and V–IX. The next barrier at 1765 cm^{-1} separates II and V from VI–IX. Next, the barrier at 1725 cm^{-1} separates I from III and IV. The barrier between III and IV is so low, that it can be assumed that under the experimental conditions, population in IV will be largely transferred to III. At 1483 cm^{-1}, a barrier separates VI from VII–IX and at 1377 cm^{-1}, the barrier between II and V is reached. The last two relevant barriers are at 944 and 713 cm^{-1}, which separate VII, VIII and IX. The barrier between VIII and IX is so low, that it is likely that in the experiment, the population from VIII is transferred to IX. The resulting populations are 14, 29, 11, 4, 5, 23, 6, 3 and 4% for conformers I–IX, respectively. Interestingly, the conformer second highest in energy, conformer II, is predicted to be most populated while the lowest energy conformer I is predicted to have a lower population than II and VI. The reason can be found in the comparatively slow increase of the density of states as a function of energy. This can be attributed to the strong internal hydrogen bonding, which makes the molecule less floppy and causes higher vibrational frequencies for the low frequency modes.

In Fig. 9, the calculated intensity distribution is compared to experimental intensity patterns, obtained after UV R2PI detection and employing neon (top) or argon (bottom) as the molecular beam expansion gas. The assignments of calculated structure to experimental R2PI peaks are the same as in Fig. 4. Structure V does not have an experimental counterpart and is shown for comparison to the right of the spectrum. The calculated intensity for VIII and IX as well as III and IV are added up, as the barriers between those respective structures are small. Considering the crudeness of the model and the uncertainties in the computed parameters (relative energies, vibrational frequencies and state densities), the agreement is surprising. Also, it should be noted that the experimental spectrum does not necessarily reflect the neutral populations, since parameters such as Franck–Condon factors, absorption cross sections and excited (intermediate) state lifetimes will affect the observed distributions. The largest discrepancy is between the experimental abundances of conformers A and E and the predicted abundances for VII, VIII and IX, which are observed to be much more intense than predicted.

A shortcoming of the calculations is that only the nine structures I–IX are considered. Other structures appear to be high in energy (see Table 1) and therefore at first glance possibly not important for the observed conformer distribution. However, when calculating the populations, energies as high as 3740 cm^{-1} are considered. At those energies, many more structures than the nine considered are expected to be populated. Those structures could significantly add to the density of states for particular types of structures and, while not populated at lower energies, act as funnels for other structures. In order to account for that, all structures that are in the range of up to the highest barrier in Fig. 7 (3740 cm^{-1}) as well as the relevant transition states would need to be considered. While in principle possible, it is not clear if the results would justify the effort.

Two striking differences between the two experimental R2PI spectra in Fig. 9 are observed. First, in the spectrum using argon as a carrier gas, small additional peaks are observed to the low energy side of conformer D. Their origin is likely the excitation of complexes with argon atoms, which subsequently dissociate, leaving an imprint of the spectrum of the argon complex on the spectrum of plain phenylalanine. Second, and more interesting, is the observation of variations in the relative intensities of conformers A and E. When using argon as a carrier gas, conformer E is much depleted and A increased, resulting in an intensity pattern that is more similar to the previous R2PI spectrum of Simons *et al.*[4] A similar observation for phenylalanine has recently been made by others.[33] It is known that the nature of the carrier gas can affect conformer distributions, and a general explanation has been given recently and illustrated with the conversion between two conformers of the weakly bound benzene dimer catalyzed by the interaction with rare gas atoms.[34] In this model, the binding energy of the rare gas atom to the molecule in a short lived collision complex is temporarily used to overcome barriers. Such a model is likely applicable here as well. The barrier for conversion of IX (the assignment for E) to VII (the assignment for A) is at 369 cm^{-1} the lowest barrier for the conformers considered. It seems possible that the binding energy of phenylalanine to argon is as large or even larger. If that is the case, a short lived collision complex of phenylalanine with an argon atom, somewhere in the expansion, would provide enough energy to overcome this barrier, effectively catalyzing the conversion from E to A.

4. Conclusions

The experimental mid-IR spectra of six conformers of phenylalanine in the gas phase are presented. All spectra are distinctively different and reveal important information on the structures of the molecules. The experimental spectra are compared to spectra calculated at the B3LYP and at the MP2 levels, based on structures proposed previously.[24] The differences between B3LYP and MP2 IR spectra are found to be small. The agreement between experiment and theory is found to be, in general, very good, however strong discrepancies exist when $-NH_2$ out-of-plane vibrations are involved, which are caused by the strongly anharmonic potential in this coordinate. In addition, transition states connecting some of the minimum structures are calculated. The relative energies of the minima as well as of the transition states are explored at the CCSD(T) level. Most transition states are found to be less than 2000 cm^{-1} above the lowest energy structure. A simple model to describe the observed conformer abundances based on quasi-equilibria near the barriers is presented and it appears to describe the experimental observation reasonably well. In addition, the vibrations of one conformer are investigated using the correlation-corrected vibrational self-consistent field method. It is found that for many modes, the anharmonic corrections are small. Larger effects are observed for N–H and O–H stretching modes.

Acknowledgements

We gratefully acknowledge the support by the Stichting voor Fundamenteel Onderzoek der Materie (FOM) in providing the required beam time on FELIX and highly appreciate the skilful assistance by the FELIX staff, in particular Dr B. Redlich and Dr A. F. G. van der Meer. Support by the Deutsche Forschungsgemeinschaft in the framework of the SFB 450 project, "Analysis and control of ultrafast photo-induced reactions" is gratefully acknowledged.

References

1 E. G. Robertson and J. P. Simons, *Phys. Chem. Chem. Phys.*, 2001, **3**, 1–18.
2 D. B. Teplow, N. D. Lazo, G. Bitan, S. Bernstein, T. Wyttenbach, M. T. Bowers, A. Baumketner, J. E. Shea, B. Urbanc, L. Cruz, J. Borreguero and H. E. Stanley, *Acc. Chem. Res.*, 2006, **39**, 635–645.
3 T. R. Rizzo, Y. D. Park, L. A. Peteanu and D. H. Levy, *J. Chem. Phys.*, 1986, **84**, 2534–2541.
4 L. C. Snoek, E. G. Robertson, R. T. Kroemer and J. P. Simons, *Chem. Phys. Lett.*, 2000, **321**, 49–56.
5 F. Dong and R. E. Miller, *Science*, 2002, **298**, 1227–1230.
6 E. Nir, C. Janzen, P. Imhof, K. Kleinermanns and M. S. de Vries, *Phys. Chem. Chem. Phys.*, 2002, **4**, 732–739.
7 L. C. Snoek, R. T. Kroemer, M. R. Hockridge and J. P. Simons, *Phys. Chem. Chem. Phys.*, 2001, **3**, 1819–1826.
8 J. M. Bakker, L. Mac Aleese, G. Meijer and G. von Helden, *Phys. Rev. Lett.*, 2003, **91**, 203003.
9 M. Gerhards and C. Unterberg, *Phys. Chem. Chem. Phys.*, 2002, **4**, 1760–1765.
10 J. M. Bakker, C. Plutzer, I. Hunig, T. Haber, I. Compagnon, G. von Helden, G. Meijer and K. Kleinermanns, *ChemPhysChem*, 2005, **6**, 120–128.
11 W. Chin, F. Piuzzi, I. Dimicoli and M. Mons, *Phys. Chem. Chem. Phys.*, 2006, **8**, 1033–1048.
12 T. M. Korter, R. Balu, M. B. Campbell, M. C. Beard, S. K. Gregurick and E. J. Heilweil, *Chem. Phys. Lett.*, 2006, **418**, 65–70.
13 B. M. Fischer, M. Hoffmann, H. Helm, R. Wilk, F. Rutz, T. Kleine-Ostmann, M. Koch and P. U. Jepsen, *Opt. Express*, 2005, **13**, 5205–5215.
14 H. Fricke, A. Gerlach and M. Gerhards, *Phys. Chem. Chem. Phys.*, 2006, **8**, 1660–1662.
15 D. Oepts, A. F. G. van der Meer and P. W. Van Amersfoort, *Infrared Phys. Tech.*, 1995, **36**, 297–308.
16 B. C. Dian, A. Longarte, S. Mercier, D. A. Evans, D. J. Wales and T. S. Zwier, *J. Chem. Phys.*, 2002, **117**, 10688–10702.
17 B. Dian, J. Clarkson and T. Zwier, *Science*, 2004, **303**, 1169–1173.
18 M. G. H. Boogaarts, G. von Helden and G. Meijer, *J. Chem. Phys.*, 1996, **105**, 8556–8568.
19 R. H. Page, Y. R. Shen and Y. T. Lee, *J. Chem. Phys.*, 1988, **88**, 4621–4636.
20 R. H. Page, Y. R. Shen and Y. T. Lee, *J. Chem. Phys.*, 1988, **88**, 5362–5376.
21 T. S. Zwier, *J. Phys. Chem. A*, 2001, **105**, 8827–8839.
22 S. J. Martinez, J. C. Alfano and D. H. Levy, *J. Mol. Spectrosc.*, 1992, **156**, 421–430.
23 K. T. Lee, J. Sung, K. J. Lee, Y. D. Park and S. K. Kim, *Angew. Chem., Int. Ed.*, 2002, **41**, 4114–4117.
24 Y. H. Lee, J. W. Jung, B. Kim, P. Butz, L. C. Snoek, R. T. Kroemer and J. P. Simons, *J. Phys. Chem. A*, 2004, **108**, 69–73.
25 A. Kaczor, I. D. Reva, L. M. Proniewicz and R. Fausto, *J. Phys. Chem. A*, 2006, **110**, 2360–2370.
26 Z. J. Huang, W. B. Yu and Z. J. Lin, *J. Mol. Struct.*, 2006, **758**, 195–202.
27 H. Piest, G. von Helden and G. Meijer, *J. Chem. Phys.*, 1999, **110**, 2010–2015.
28 R. A. Kydd and P. J. Krüger, *Chem. Phys. Lett.*, 1977, **49**, 539–543.
29 A. P. Scott and L. Radom, *J. Phys. Chem.*, 1996, **100**, 16502–16513.
30 J. O. Jung and R. B. Gerber, *J. Chem. Phys.*, 1996, **105**, 10332.
31 G. M. Chaban, J. O. Jung and R. B. Gerber, *J. Chem. Phys.*, 1999, **111**, 1823.
32 B. Brauer, G. M. Chaban and R. B. Gerber, *Phys. Chem. Chem. Phys.*, 2004, **6**, 2543–2556.
33 T. Ebata, T. Hashimoto, T. Ito, Y. Inokuchi, F. Altunsu, B. Brutschy and P. Tarakeshwar, *Phys. Chem. Chem. Phys.*, 2006, **8**, 4783–4791.
34 U. Erlekam, M. Frankowski, G. von Helden and G. Meijer, *Phys. Chem. Chem. Phys.*, 2007, **9**, 3786–3789.

